

# COSMOLOGY, COSMOMICROPHYSICS AND GRAVITATION

## THE DISTRIBUTION OF BARYON MATTER IN THE NEARBY X-RAY GALAXY CLUSTERS

Iu.V. Babyk<sup>1,2,3</sup>, I.B. Vavilova<sup>1</sup>

<sup>1</sup> Main Astronomical Observatory of NAS of Ukraine, Kyiv, Ukraine

<sup>2</sup> Dublin Institute for Advanced Studies, Dublin, Ireland

<sup>3</sup> Dublin City University, Dublin, Ireland,  
*babikyura@gmail.com, irivav@mao.kiev.ua*

**ABSTRACT.** We present the results on the distribution of baryon matter in the galaxy clusters ( $z < 0.2$ ), based on the *Chandra* X-ray Observatory data. The observed surface brightness profiles were approximated by  $\beta$ -model, which provides a good fit for all clusters. We found a correlation between cluster's radius  $R_{200}$  and temperature  $T$ , taking into account that their measurements are statistically independent because of the mass of gas is almost independent on cluster's temperature:  $R_{200} = 850 \text{ kpc} \times T^{0.61 \pm 0.04} \text{ keV}$ . We obtained an empirical relation for a total mass of baryon matter (intercluster medium and galaxies), and the upper limit (25-30%) on its changes in a total mass of nearby X-ray galaxy clusters.

**Key words:** Galaxy clusters: X-ray galaxy clusters.

### 1. Sample and data processing

To analyze the evolution of the baryon mass function of galaxy clusters we should provide relevant measurements for galaxy clusters at all redshifts, including the small ones. With this aim and to reveal the distribution of visible/dark matter we compiled a sample of 34 X-ray nearby galaxy clusters ( $z < 0.2$ ). These clusters were selected from a larger sample of *Chandra* X-ray galaxy clusters ( $0.01 < z < 1.5$ ), which is described fully in our previous work (Babyk, Vavilova, Del Popolo, 2012 (hereafter BVP sample)). The main criteria were that clusters should be sufficiently symmetrical and each X-ray cluster image should trace the surface brightness profile at larger as possible radii. To satisfy the second statement we selected clusters with a wide exposure interval (not less 5000 s) and, moreover, under the condition that a virial radius fits on the line of sight. The value of a virial radius was taken as  $R_{200}$  (a providing accuracy is sufficient for the purposes of our study). Following these criteria, we excluded A754, A1750, A2151, etc clusters from our BVP sample, nevertheless that are at  $z < 0.2$ , because of their irregular morphology or double structure. Our sample of 34 nearby X-ray galaxy clusters is given in Tab. 1.

In fact, there is a question, how to remove all sources where a width response function strongly increases at large deviations from the optical axis, resulting in the center and on the end of the images of pointed source's focuses of a different future intensity of a cosmic X-ray background.

Nevertheless, we decided to eliminate all such sources, but after checking we found that it does not affect significantly the results contributing only to reduction of a non-static background in the obtained brightness profiles (see Babyk et al., 2012; Babyk, 2012a; Babyk, 2012; Babyk, Vavilova, 2012).

We have measured the brightness profiles in concentric rings of equal logarithmic width, which were centered on the cluster's maximum brightness; the radii's ratio of inner and outer rings is equal to 1.1. We have used two types of profiles: the average azimuthal brightness profiles and profiles in six angle sectors  $0 - 60, \dots, 300 - 360$ . It allowed us to verify the choice of other "reasonable" centroid profiles: the measured surface brightness distribution at large radii were practically identical.

As for a cosmic X-ray background, we have measured it individually for each cluster because of a significant contribution to the overall brightness of X-ray galaxy cluster may occur even at large distances from the center. Usually, the X-ray cluster's surface brightness is about 5-20% of the background near the radius  $R_{200}$ . Since, in many cases, this radius is a quite close to the size of the telescope's field of view, it is practically impossible to isolate the studied image for a direct determination of the background level.

Thus, we have considered that the surface brightness cluster radius at large radii should follow the exponential law, and therefore the observation surface brightness could be approximated as  $Ar^{-\gamma} + const$ . Thus, this approximation in the range of radii  $r > R_{200}/3$  allows us to find the intensity level of the background. According to the observations of distant clusters, in which the level of background can be measured directly, we verified that this method gives the correct result.

Finally, using observations of blank fields, we checked the images alignment quality: the difference between the background level in the center and on the end of the image does not exceed  $\sim 5\%$  after eliminating all the sources. We notice that this 5% variation in the background levels gives an additional uncertainty of  $\beta$ - parameter of the  $\beta$ - model at  $\delta\beta \sim 0.3 - 0.4$  and 2.1% uncertainty in the value of  $R_\delta$ . We used the cosmological parameters  $H_0 = 73$  km/s/Mpc,  $\Omega_M = 0.27$ , and  $\Omega_\Lambda = 0.73$  in our study.

## 2. X-ray galaxy clusters surface brightness profiles: methods

### 2.1. Modeling the surface brightness profiles

We used the *Sherpa* software package and  $\beta$ - model (Cavaliere, Fusco-Femiano, 1976) to determine the galaxy cluster brightness profiles:

$$S(r) = S_0(1 + r^2/r_c^2)^{-3\beta+0.5}, \quad (1)$$

$S_0, r_c$  and  $\beta$  are the free parameters. Such a model was used firstly by (Jones, Forman, 1999,) when analyzing the images of galaxy clusters based on the data from “Einstein” X-ray space observatory. The value of  $\beta$  for those clusters was in the range from 0.5 to 0.8 (the better value is 0.67). The authors noticed also a non-significant correlation between  $\beta$  - parameter and temperature of clusters: X-ray clusters with a higher temperature have a higher value of  $\beta$  - parameter.

The numerical simulations of that times provided more steeper profiles of density matter distribution, and  $\beta \approx 0.8 - 1$  (see, for example, Navarro, Frenk, White, 1998), which was contrary to the observations. Bartelmann and Steinmetz (1996) argued that the surface brightness profiles may curl at the larger radii but we can not observe such a process because the brightness of cluster is decreasing due to the influence of background. They proposed to check an accuracy of modeling of brightness profiles using  $\beta$ - model, because it allows to determine the mass of cluster under the condition of the hydrostatic equilibrium of intracluster gas (Hoekstra, 2007). We decided to apply a simple  $\beta$ -model for analyzing the observational surface brightness profiles in the studied nearby X-ray clusters as well as to clear up how such a procedure likely the azimuthal corrections of surface brightness profiles in galaxy clusters is fair one.

### 2.2. Excluding the cold galaxy cluster’s centers

The most number of X-ray clusters with a normal morphology consists of a strong central peak of surface brightness, which is usually explained as a consequence of radiative cooling of the gas. Using the central parts of such clusters the approximation by  $\beta$ - model leads to the small values of the core radius  $r_c$  and  $\beta$ - parameter as well as to the weak data approximation in

general. Obviously, a central part of the X-ray galaxy cluster images must be excluded during their processing, if the aim of a study concerns with a correct analysis of the gas distribution at large cluster’s radii.

There are several approaches to this problem. For example, Jones, Forman (1999) increased gradually a value of the minimal radius until the approximation of the surface brightness profile not leads to the acceptable values of  $\chi^2$ . A new method to resolve such a problem is concerns with the search of the required radius parameter while a gas radiative cooling does not affect the distribution of a gas in the galaxy cluster till a typical value of a gas cooling time not exceeds the age of the Universe. Such a method, where a gas radiative cooling parameter described in a value of the radius  $R_{col}$ , and a gas radiative cooling time is  $1.3 \times 10^{10}$  years, was introduced and analysed by White, Fabian (1995), Peres et al. (1998). Taking into account these results and the aforementioned analytical approximation we calculated  $R_{col}$  parameter and excluded range of radii  $r < R_{col}$  for each cluster from our sample.

### 2.3. The slope of surface brightness profile at the large radii

Our results on the approximation of surface brightness profiles are given in Tab. 1. The values obtained for the nuclei radii  $r_c$  are often comparable with the  $R_{col}$  parameter in the case of clusters with the central peaks of a surface brightness, indicating thus that  $r_c$  can not be reliably measured. Meanwhile, the value of  $\beta$ - parameter is measured accurately and reliably as well as such an approximation responds well to the observations.

The obtained values of  $\beta$ - parameter are shown in Fig. 2. If we compare these values with those from the work by Jones, Forman (1999), where  $\beta$ - parameter had a fairly narrow range  $0.7 \pm 0.1$ , we may conclude as follows from Fig. 2: only a few nearby *Chandra* X-ray clusters from our sample have  $\beta < 0.6$ .

As concerns with the question on the correlation between  $\beta$ - parameter and cluster’s temperature  $T$  (left panel in Fig. 2). Our analysis allows to conclude that the previous statement about the absence of  $\beta$ - $T_X$  correlation was based on the small values of  $\beta \sim 0.5$  for the cold X-ray clusters ( $T \sim 3$  keV), which are characterized by the steeper surface brightness profiles. The most likely explanation for this discrepancy is related to the incomplete removal of the cooling central parts during processing the data on X-ray clusters in earlier works. We considered the same radial range (by the coordinate’s position):  $0.3R_{200}(T) < R < 1.5R_{200}(T)$ . The nuclei  $r_c$  parameter can not be determined in this range from the *Chandra* data, so we fixed it at  $0.1R_{200}$  or at the value that was obtained in the entire range of radii during approximation. Since  $r_c$  is usually much less than  $0.3R_{200}(T)$ , so the data approximation is equivalent to the application of a power law model,

$$S \sim r^{-6\beta+1}.$$

The obtained values of  $\beta_{out}$  are given in Tab. 1 and are presented dependently on the cluster's temperature  $T$  in Fig. 2 (right panel). The measured slope of a surface brightness profile in the outer part of this Figure was slightly steeper than it follows from approximating  $\beta$ -model across the range of radii. An extreme case is related to the A2163 cluster, where  $\beta$  is changed to 0.17. The swirled surface brightness profile of the A2163 at  $r > 0.3R_{200}(T)$  is obvious (Fig. 2). We notice that the changes of  $\beta$  in the outer parts of the clusters are much smaller,  $\Delta\beta \approx 0.05$ , as well as are not statistically significant for the most of galaxy clusters of our sample.

Thus, we concluded on the correlation between  $\beta_{out}$  parameter and cluster's temperature  $T$ . It is caused mainly by a group of five hot ( $T = 6$ -10 keV) clusters (A85, A401, A478, A644, A1413, etc.) with  $\beta > 0.7$ , as well as by a strong twist profile of the hottest A2163 cluster. However, one can see from Fig. 2 that there are systematic changes in the slope of surface brightness profile at the large radii of clusters, which are within the scatter at the high temperatures. We notice that the observed trend is a weak for  $\beta \approx 0.67$  for clusters with  $T = 3$  keV to  $\beta \approx 0.7$ -0.75 with  $T = 10$ -13 keV.

#### 2.4. Azimuthal variations of the surface brightness profile

Here we consider the question how the procedure of an azimuthal averaging of the surface brightness profile has been applied to the study of the intergalactic gas distribution at the large radii. With this aim we have compared the values of  $\beta_{out}$ , measured in the angle sectors  $0 - 60, \dots, 300 - 360$ . The presence of azimuthal variations of  $\beta_{out}$  means a cluster's irregularity.

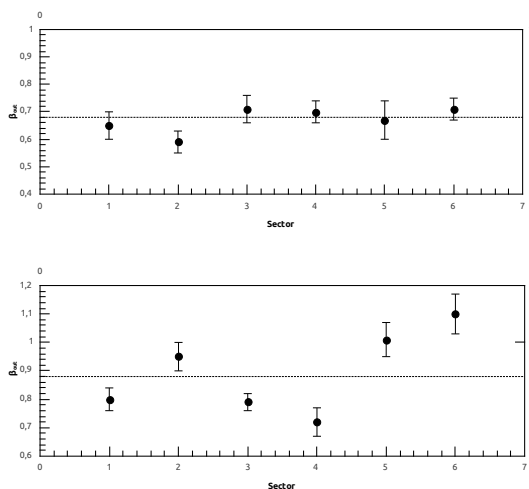


Figure 1: The azimuthal variations of  $\beta_{out}$  in the galaxy clusters 2029 (top) and 1795 (down).

We found that our sample contains both the symmetrical clusters (likely A2029) and the clusters with significant variations in the slope in the outer part (likely A1795) (see, Fig. 1), but these variations in the slope are small in general. The values of all azimuthal variations  $\beta_{out}$  in the studied clusters are given in Tab. 1. In the most cases they are less than 0.1 and demonstrate often a strong deviation in a single sector. Thus, we may conclude about the absence of the major errors through the azimuthal averaging brightness profiles in the outer parts of the studied clusters.

### 3. The intracluster gas density distribution

Under the condition of spherical symmetry of the cluster and the observed surface brightness profile we can find the volume of emitting ability, which is then easily transferred to the gas density profile, using the fact that the plasma radiating capacity in the soft X-ray range is proportional to the square of the density and dependent very weakly on the temperature (Einasto, 2001).

#### 3.1. The correlation between radius of contrast of density baryons and temperature of cluster galaxy

The theory of the formation of clusters provides correlation between mass and temperature of clusters,  $M \sim T^{3/2}$ . Since the mass and radius corresponding to this density contrast associated as  $M_{200} \sim R_{200}^3$ , we can expect the following correlation  $R_{200}$  and temperature:  $R_{200} \sim T^{1/2}$ . Since most of the baryons are concentrated in the X-ray intergalactic gas, this ratio ( $R_{200} - T_X$ ) for baryons can be easily verified.

The contrast of baryon density is defined as the ratio of the mass of gas within a certain radius and the value of  $(4\pi/3)\rho_0 R^3(1+z)^3$ , where  $\rho_0$  is the current density of baryons in the Universe. This compares reliably the relative content of light elements from the theory of primary nucleosynthesis,  $\rho_0 = (5.55 \pm 0.28) \times 10^9 M_\odot \text{Mpc}^{-3}$ . Radius  $R_{200}$  is sufficiently close to the virial radius  $r_{vir}(T)$ . Correlation between the cluster's radius  $R_{200}$  and temperature  $T$  is shown in Fig. 3. We notice that since the measurement of the mass of gas is almost independent of temperature clusters, measuring  $R$  and  $T$  are also statistically independent.

The observed correlation has a small scatter and close to the theoretically expected correlation of  $R \sim T^{0.5}$ . Note, that even A3391 with abnormally flat surface brightness profile is well accumulated within the average dependence. The measured correlation  $R_{200} - T_X$  was modeled (Akritas, Bershadsky, 1996) using a power law model that allowed us also to consider both statistical and internal variations in the data on both axes.

Table 1: The sample and results of approximation of the surface brightness profiles of galaxy clusters on  $z < 0.2$  using  $\beta$ - model.

| Name  | T,<br>(keV)             | z,    | R <sub>200</sub> ,<br>(Mpc) | $\beta$ ,       | $\beta_{out}$ , | $r_c$ ,<br>(kpc) |
|-------|-------------------------|-------|-----------------------------|-----------------|-----------------|------------------|
| A13   | $5.76^{+0.15}_{-0.15}$  | 0.094 | $1.51^{+0.47}_{-0.33}$      | $0.65 \pm 0.08$ | $0.68 \pm 0.03$ | $84 \pm 8$       |
| A85   | $6.20^{+0.40}_{-0.15}$  | 0.055 | $2.71^{+0.65}_{-0.73}$      | $0.75 \pm 0.03$ | $0.76 \pm 0.03$ | $374 \pm 54$     |
| A119  | $5.71^{+0.16}_{-0.15}$  | 0.044 | $2.66^{+0.13}_{-0.15}$      | $0.64 \pm 0.06$ | $0.61 \pm 0.04$ | $342 \pm 49$     |
| A400  | $2.33^{+0.21}_{-0.17}$  | 0.024 | $1.55^{+0.24}_{-0.13}$      | $0.55 \pm 0.07$ | $0.58 \pm 0.03$ | $185 \pm 20$     |
| A401  | $8.16^{+0.87}_{-0.78}$  | 0.074 | $3.07^{+1.21}_{-0.99}$      | $0.63 \pm 0.07$ | $0.69 \pm 0.02$ | $267 \pm 51$     |
| A478  | $6.90^{+0.35}_{-0.35}$  | 0.088 | $2.60^{+0.41}_{-0.55}$      | $0.75 \pm 0.04$ | $0.80 \pm 0.06$ | $311 \pm 30$     |
| A496  | $4.89^{+0.12}_{-0.14}$  | 0.033 | $1.93^{+0.48}_{-0.35}$      | $0.70 \pm 0.06$ | $0.75 \pm 0.03$ | $237 \pm 22$     |
| A539  | $3.33^{+0.29}_{-0.31}$  | 0.028 | $1.88^{+0.33}_{-0.18}$      | $0.69 \pm 0.03$ | $0.73 \pm 0.04$ | $244 \pm 33$     |
| A644  | $6.59^{+0.17}_{-0.17}$  | 0.070 | $2.92^{+0.77}_{-0.81}$      | $0.71 \pm 0.03$ | $0.71 \pm 0.04$ | $244 \pm 41$     |
| A780  | $4.33^{+0.15}_{-0.18}$  | 0.054 | $1.69^{+0.48}_{-0.37}$      | $0.65 \pm 0.08$ | $0.61 \pm 0.04$ | $119 \pm 25$     |
| A1413 | $6.77^{+0.36}_{-0.26}$  | 0.14  | $1.83^{+0.66}_{-0.57}$      | $0.68 \pm 0.01$ | $0.70 \pm 0.02$ | $219 \pm 17$     |
| A1651 | $6.11^{+0.20}_{-0.21}$  | 0.085 | $2.45^{+0.46}_{-0.37}$      | $0.70 \pm 0.02$ | $0.77 \pm 0.04$ | $256 \pm 43$     |
| A1689 | $9.02^{+0.40}_{-0.30}$  | 0.183 | $2.23^{+0.03}_{-0.07}$      | $0.75 \pm 0.05$ | $0.81 \pm 0.06$ | $265 \pm 64$     |
| A1795 | $6.88^{+0.14}_{-0.14}$  | 0.063 | $2.46^{+0.36}_{-0.54}$      | $0.77 \pm 0.06$ | $0.88 \pm 0.07$ | $377 \pm 48$     |
| A2029 | $8.45^{+0.47}_{-0.45}$  | 0.077 | $2.94^{+0.96}_{-0.82}$      | $0.68 \pm 0.03$ | $0.66 \pm 0.04$ | $277 \pm 74$     |
| A2052 | $3.22^{+0.22}_{-0.22}$  | 0.035 | $1.93^{+0.55}_{-0.61}$      | $0.64 \pm 0.03$ | $0.66 \pm 0.03$ | $133 \pm 35$     |
| A2063 | $4.21^{+0.55}_{-0.36}$  | 0.035 | $2.01^{+0.45}_{-0.37}$      | $0.68 \pm 0.02$ | $0.69 \pm 0.04$ | $210 \pm 45$     |
| A2124 | $10.88^{+1.78}_{-2.01}$ | 0.065 | $2.16^{+0.63}_{-0.61}$      | $0.67 \pm 0.03$ | $0.59 \pm 0.04$ | $254 \pm 73$     |
| A2142 | $9.57^{+0.92}_{-1.11}$  | 0.091 | $2.82^{+0.59}_{-0.61}$      | $0.75 \pm 0.05$ | $0.73 \pm 0.04$ | $387 \pm 47$     |
| A2163 | $14.01^{+1.89}_{-1.45}$ | 0.203 | $4.22^{+0.68}_{-0.66}$      | $0.73 \pm 0.04$ | $0.87 \pm 0.04$ | $417 \pm 36$     |
| A2199 | $4.15^{+0.23}_{-0.21}$  | 0.030 | $2.14^{+0.28}_{-0.19}$      | $0.64 \pm 0.03$ | $0.67 \pm 0.05$ | $155 \pm 25$     |
| A2218 | $7.39^{+1.03}_{-0.89}$  | 0.175 | $1.65^{+0.16}_{-0.12}$      | $0.66 \pm 0.03$ | $0.71 \pm 0.03$ | $234 \pm 46$     |
| A2255 | $7.30^{+1.20}_{-1.20}$  | 0.081 | $3.21^{+0.46}_{-0.27}$      | $0.74 \pm 0.04$ | $0.73 \pm 0.06$ | $552 \pm 37$     |
| A2256 | $7.53^{+0.91}_{-0.75}$  | 0.058 | $3.33^{+0.62}_{-0.58}$      | $0.72 \pm 0.03$ | $0.75 \pm 0.04$ | $436 \pm 57$     |
| A2462 | $2.55^{+0.71}_{-0.66}$  | 0.073 | $2.51^{+0.27}_{-0.22}$      | $0.65 \pm 0.03$ | $0.66 \pm 0.04$ | $221 \pm 36$     |
| A2597 | $4.39^{+0.45}_{-0.51}$  | 0.085 | $2.01^{+0.57}_{-0.73}$      | $0.66 \pm 0.03$ | $0.66 \pm 0.04$ | $166 \pm 45$     |
| A2657 | $3.77^{+0.81}_{-0.77}$  | 0.040 | $1.98^{+0.15}_{-0.11}$      | $0.75 \pm 0.05$ | $0.73 \pm 0.02$ | $372 \pm 40$     |
| A2717 | $2.31^{+0.34}_{-0.15}$  | 0.049 | $2.16^{+0.79}_{-0.81}$      | $0.68 \pm 0.03$ | $0.66 \pm 0.02$ | $71 \pm 3$       |
| A3112 | $4.86^{+0.56}_{-0.67}$  | 0.075 | $2.43^{+0.31}_{-0.26}$      | $0.61 \pm 0.04$ | $0.65 \pm 0.03$ | $119 \pm 12$     |
| A3391 | $7.01^{+0.63}_{-0.73}$  | 0.051 | $2.45^{+0.84}_{-0.35}$      | $0.55 \pm 0.01$ | $0.56 \pm 0.03$ | $210 \pm 17$     |
| A3571 | $8.21^{+0.86}_{-0.73}$  | 0.039 | $2.88^{+0.46}_{-0.37}$      | $0.69 \pm 0.03$ | $0.61 \pm 0.05$ | $271 \pm 32$     |
| A4038 | $3.32^{+0.53}_{-0.42}$  | 0.030 | $1.87^{+0.25}_{-0.17}$      | $0.60 \pm 0.04$ | $0.61 \pm 0.03$ | $162 \pm 43$     |
| A4059 | $4.11^{+0.35}_{-0.32}$  | 0.047 | $2.03^{+0.28}_{-0.34}$      | $0.65 \pm 0.04$ | $0.66 \pm 0.03$ | $222 \pm 48$     |
| AWM4  | $2.44^{+0.19}_{-0.25}$  | 0.032 | $1.73^{+0.27}_{-0.22}$      | $0.62 \pm 0.04$ | $0.67 \pm 0.07$ | $125 \pm 42$     |

The variation has value only 5.5% for  $R_{200}$  at this temperature. Although the obtained slopes differ formally from the theoretical value of 0.5 for  $2 - 3\sigma$ , the discrepancy between the best approximation and the power law  $R \sim T^{0.5}$  lies completely within the scatter of data. The resulting ratio is as follows:

$$R_{200} = 850 \text{ kpc} \times T^{0.61 \pm 0.04} \text{ keV} \quad (2)$$

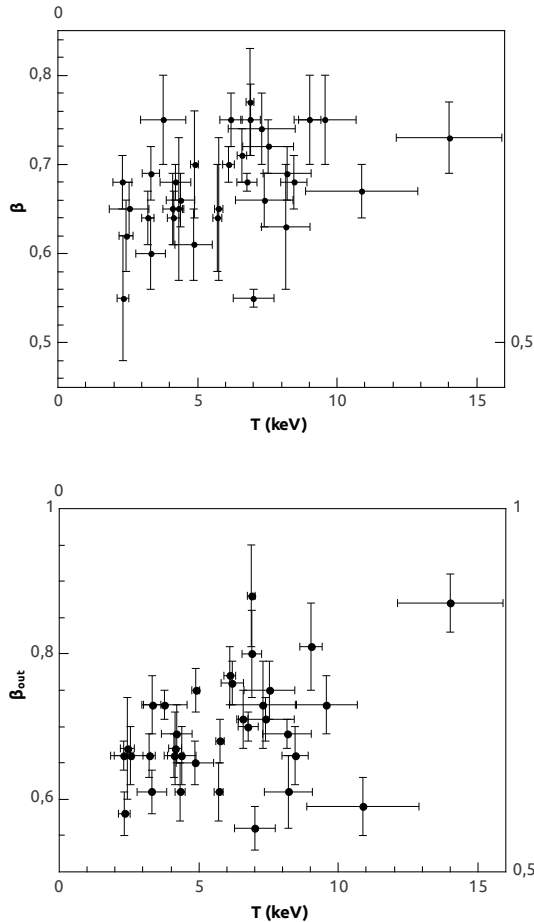


Figure 2: The correlation between  $\beta$  and temperature of galaxy clusters. Top:  $\beta$  is taken from approximation at all range of radii. Down:  $\beta$  is taken from approximation at  $0.3R_{200} < R < 1.5R_{200}$ .

Main difference with other relations, such as luminosity-temperature or size-temperature, are related to the fact that the data, which are depending on the parameters of concentrated gas distribution, were obtained from the inner parts of cluster, but the correlation between  $R_{200}$  and  $T$  was obtained based on the data from the outer parts. So, the properties of the central parts of clusters can strongly affect various non-gravitational processes, which are not important at large radii, where the main part of the cluster's mass is concentrated.

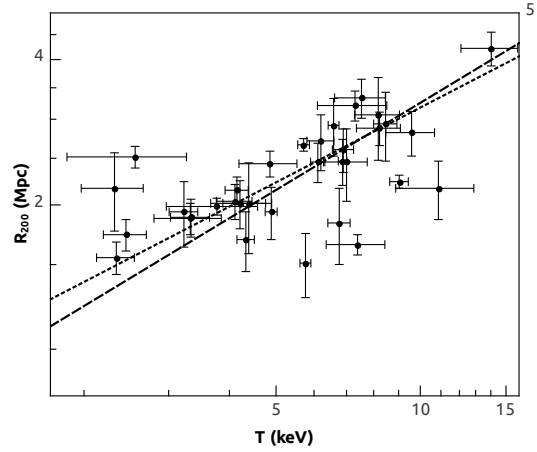


Figure 3: The correlation of  $R_{200}$  and temperature clusters. Dotted line shows approximations with power law model, and dashed line shows theoretical model from correlation  $R \sim T^{0.5}$ .

### 3.2. The upper limit on the changes of baryons in total mass of galaxy clusters

Small scatter observed in the correlation  $R_{200} - T$  can help us to find upper limit on variation in the proportion of baryons in total mass between different clusters and its systematic dependence on temperature. We used the theoretically expected fact that the total mass of the cluster within a radius of density contrast correlated with temperature as  $M_{tot} \sim T^{3/2}$ . Observed ratio for baryons,  $R \approx \text{const} \times T^{1/2}$  is equivalent  $M_{gas} \sim T^{3/2}$ . It means that  $f_{gas} = M_{gas}/M_{tot} \approx \text{const}$ . Since the hot gas is the dominant baryon component in clusters, we can conclude that the proportion of baryons in total mass is constant too. The best approximation is  $R_{200} \sim T^{0.57}$  and corresponds to a small change in gas content in total mass:  $f_{gas} \sim T^{0.2}$ . However, if we consider the fraction of stars in the mass of baryons, which is higher in cold clusters, then this trend is significantly reduced and we can count that for wide range of temperatures the fraction of baryon mass in total mass of clusters is constant.

We now consider possible the variations of  $f_{gas}$  between different clusters with a given temperature. In the outer parts of the clusters radial correlation of the contrast density of gas is  $\delta \sim r^{-3\beta}$ . Accordingly, the observed 6.5%-variations within the fixed  $\delta_{gas}$  corresponds to approximately  $3\beta \times 6.5\%$  variation of contrast at a given radius. Hence, we can predict that the total mass of clusters clearly related to temperature.

In fact, the ratio  $M_{tot} - T$  has scatter of  $f_{gas}$  for clusters with a given mass of somewhat reduced. Thus, the findings suggest that the contribution of baryons in the total mass is constant, the same for different clusters of galaxies, and is independent from their temperature.

#### 4. The total mass of baryons and the upper limit on its changes in the nearby X-ray clusters

We now consider possible the variations of  $f_{gas}$  between different clusters with a given temperature. The radial correlation of the contrast density of gas is  $\delta \sim r^{-3\beta}$  in the outer parts of clusters. Accordingly, the observed 6.5%-variations within the fixed  $\delta_{gas}$  correspond to approximately  $3\beta \times 6.5\%$  variation of contrast at a given radius. Hence, we can predict that the total mass of clusters clearly related to the temperature. In fact, the ratio  $M_{tot} - T$  has the scatter of  $f_{gas}$  for clusters with a given mass of somewhat reduced. Thus, we may suggest that the contribution of baryons in the total mass is constant being the same for different clusters of galaxies, and it's independent on their temperature.

Voevodkin, Vikhlinin & Pavlinskii (2002a) calculated the correlation ratio between the baryon's mass and the total X-ray luminosity of clusters. This ratio provides an opportunity to make a rough estimate of the mass in those situations when the quality of the X-ray data are not available. More importantly that an availability of  $M - L$  ratio helps to determine the volume, which is covered by the survey, with any restriction on the flow, depending on the mass of the cluster, and thus, finally, the mass function. These authors obtained also (Voevodkin, Vikhlinin & Pavlinskii, 2002b) an integral function of the baryon mass which takes into account a statistical measurement error of the mass function of close clusters as well as distortions caused by the measurement errors for the masses of individual clusters.

We measured the mass profiles of intracluster gas in all the studied galaxy clusters using *Chandra* data and aforementioned analysis. After a very accuracy applying the correlation ratio between the mass of hot gas and total optical luminosity taken from the paper by Voevodkin, Vikhlinin, Pavlinskii (2002a), we found not only the mass of gas, but also the total mass of baryons (intracluster gas + stars) for the X-ray clusters from our sample:

$$M_b = M_g \times \left[ 1.33 + 0.05 \left( \frac{M_g}{10^{15} M_\odot} \right)^{-0.52} \right] \quad (3)$$

Here,  $M_b$  is the mass of baryons at the contrast  $\delta = 200$ ,  $M_g$  is the mass of gas at the same contrast without a fraction of stars. The fraction of stars in the total mass of baryons is significant and equal  $\sim 10$ -15 % for massive clusters. Considering that the mass ratio of the gas and stars do not evolve at large  $z$  (i.e., galaxies do not associate themselves hot intergalactic gas), this ratio can be used for a measurement of the total baryonic mass of distant clusters, for which the sufficient quality optical observations are not available yet.

Thus, the baryon mass function for X-ray galaxy clusters at the small redshifts can be estimated with

the use of Eq. 3. Observations of *Chandra* distant clusters can give us an opportunity to measure the baryon mass function also at the large redshifts (see, for example, the related paper by Schmidt & Allen (2007), and on the distinguished use of this approach by Babyk, Vavilova, Del Popolo (2012)).

*Acknowledgements.* We notice on the usage of the *Chandra* Data Archive and the *Chandra* Source Catalog, and software provided by the *Chandra* X-ray Center (CXC) in the application packages *CIAO*, *ChIPS*, and *Sherpa*. This work was partially supported in frame of the "CosmoMicroPhysics" Program and the Target Project of the Physics and Astronomy Division of the NAS of Ukraine.

#### References

- Akritas M.G., Bershadsky M.A.: 1996, *ApJ*, **470**, 706.
- Babyk Iu.: 2012, *Journ. Phys. Studies*, **16**, 7.
- Babyk Iu.: 2012, *Izv. CrAO*, **108**, 127.
- Babyk Iu., Melnyk O., Elyiv A., Krivodubskij V.: 2012, *Kinemat. Physics Celest. Bodies*, **28**, 69.
- Babyk Iu., Vavilova I., Del Popolo A.: 2012, *submitted to MNRAS*, **arXiv:1208.2424**.
- Babyk Iu., Vavilova I.: 2012, *Proc. Confer. Young Scientists of CIS Countries, Armenia, 2011*, 162.
- Bartelmann M., Steinmetz M.: 1996, *MNRAS*, **283**, 431.
- Cavaliere A., Fusco-Femiano R.: 1976, *A&A*, **49**, 137.
- Einasto J.: 2001, *New Astronomy Reviews*, **45**, 355.
- Jones C., Forman W.: 1999, *ApJ*, **511**, 65.
- Hoekstra H.: 2007, *MNRAS*, **379**, 317.
- Mohr J.J., Evrard A.E.: 1997, *ApJ*, **491**, 38.
- Navarro J.F., Frenk C.S. & White S.D.: 1998, *MNRAS*, **275**, 720.
- Peres C. et al.: 1998, *MNRAS*, **298**, 416.
- Schmidt R.W., Allen S.W.: 2007, *MNRAS*, **379**, 209.
- Voevodkin A.A., Vikhlinin A.A., Pavlinskii M.N.: 2002, *Letters in AJ*, **28**, 366.
- Voevodkin A.A., Vikhlinin A.A., Pavlinskii M.N.: 2002, *Letters in AJ*, **28**, 793.
- White D.A. & Fabian A.C.: 1995, *MNRAS*, **273**, 72.